

Supplementary Materials

Article

Natural Wollastonite-Derived Two-Dimensional Nanosheet $\text{Ni}_3\text{Si}_2\text{O}_5(\text{OH})_4$ as a Novel Carrier of CdS for Efficient Photocatalytic H_2 Generation

Jiarong Ma ¹, Run Zhou ¹, Yu Tu ¹, Ruixin Ma ², Daimei Chen ^{1,*} and Hao Ding ^{1,*}

¹ Beijing Key Laboratory of Materials Utilization of Nonmetallic Minerals and Solid Wastes, National Laboratory of Mineral Materials, School of Materials Science and Technology, China University of Geosciences, Xueyuan Road, Haidian District, Beijing 100083, China; mmmjr666@163.com (J.M.); 3003180004@email.cugb.edu.cn (R.Z.); tuyu0803@126.com (Y.T.)

² School of Chemical and Environmental Engineering, North China Institute of Science and Technology, Langfang 065201, China; maruixin@126.com

* Correspondence: chendaimei@cugb.edu.cn (D.C.); 2003011690@cugb.edu.cn (H.D.)

Table of contents

Section 1. Test and characterizations.

Section 2. Photocatalytic H₂ evolution performance.

Figure S1. The XRD patterns of Ni₃Si₂O₅(OH)₄ prepared under different conditions:

(a) different mole ratios of Ni and Ca in wollastonite and (b) different reaction temperatures and times.

Figure S2. The SEM of wollastonite before the reaction.

Figure S3. The SEM of wollastonite (a): Ca (a1) and Ni (a2) element distribution of wollastonite (a); the SEM of 3-NS-200-24 (b): Ca (b1) and Ni (b2) element distribution of 3-NS-200-24 (b).

Figure S4. The band structures of CdS and Ni₃Si₂O₅(OH)₄.

Table S1. Specific surface area and pore volume of wollastonite, Ni₃Si₂O₅(OH)₄, and CdS/NS.

Section S1. Test and characterization

The X-ray powder diffraction (XRD) analysis of the samples was performed using a diffractometer (D8 Advance, Bruker Company, Germany) with a Cu target, $\lambda = 1.5418 \text{ \AA}$, $U=40 \text{ kV}$, $A=40 \text{ mA}$, and a scanning speed of $10^\circ/\text{min}$. The particle morphology, structure, and size of the samples were observed using a Gemini field emission scanning electron microscope (SEM, German ZEISS company) and high-resolution field emission transmission electron microscopy (TEM, Tecnai G2 F30, American FEI company). The specific surface area and pore structure of the samples were analyzed using the QUADRASORB SI fully automatic surface area and porosity analyzer produced by Conta Instruments in the United States. The surface functional groups of the sample were qualitatively analyzed using an infrared spectrometer (FT-IR, Spectrum One, PerkinElmer, USA). The elemental valence states of the samples were analyzed using X-ray photoelectron spectroscopy (XPS) with a Thermo escalab 250Xi instrument (Thermo Fisher, USA). The luminescence performance of the samples was characterized using a fluorescence spectrometer (F-4600, Hitachi, Japan). The photoelectric performance of the samples was tested using an electrochemical workstation (CHI760 type, Shanghai Huachen Instrument Company). For the preparation of the photoelectrode, 1 mg of the sample was dispersed in 1 mL of ethanol and sonicated for 30 minutes to obtain a suspension. The suspension was then evenly dropped onto cleaned ITO glass (50 mm in length and 20 mm in width). After natural drying, the ITO glass was placed in an oven at 120°C for 2 hours to prepare the photoelectrode. A three-electrode system was used for the test.

A platinum wire served as the counter electrode, the prepared photoelectric electrode was the working electrode, and the saturated calomel electrode was used as the reference electrode. The electrolyte used was a 0.1 mol/L Na₂SO₄ solution.

By analyzing the sample's absorption intensity at different wavelengths using UV–visible diffuse reflectance spectroscopy, and based on these data, the bandgap width spectrum (E_g) of the sample was calculated using the Kubelka–Munk function. The Kubelka–Munk function and the formula for estimating the bandgap width are, respectively, as follows:

$$F(R) = K/S = (1-R)^2/2R \quad (1)$$

where K, S, and R represent the absorption coefficient, scattering coefficient, and reflectance coefficient of the sample, respectively.

$$F(R)h\nu = A(h\nu - E_g)^m \quad (2)$$

where A is the absorption coefficient; $h\nu$ represents the photon energy, approximately $1239.8/\lambda$; and m represents the transition coefficient. The equipment used in this test was a Hitachi U-3900 UV-Vis spectrophotometer with a scanning range of 200-800 nm.

Section S2. Photocatalytic H₂ evolution performance

Firstly, 30 mg of the sample was placed inside a quartz reaction vessel. Subsequently, 90 mL of deionized water and 10 mL of lactic acid (used as the sacrificial agent) were added to the reaction vessel. The container was then purged with argon gas for 40 minutes to eliminate any air present. Once the air was completely removed, the reactor was transferred to a photoreactor for the light

reaction, with a 300 W xenon lamp serving as the light source. Hourly syringe samples were taken and injected into a gas chromatography system (GC9790 Plus, Fuli Instruments, China) to measure the content of H₂ produced.

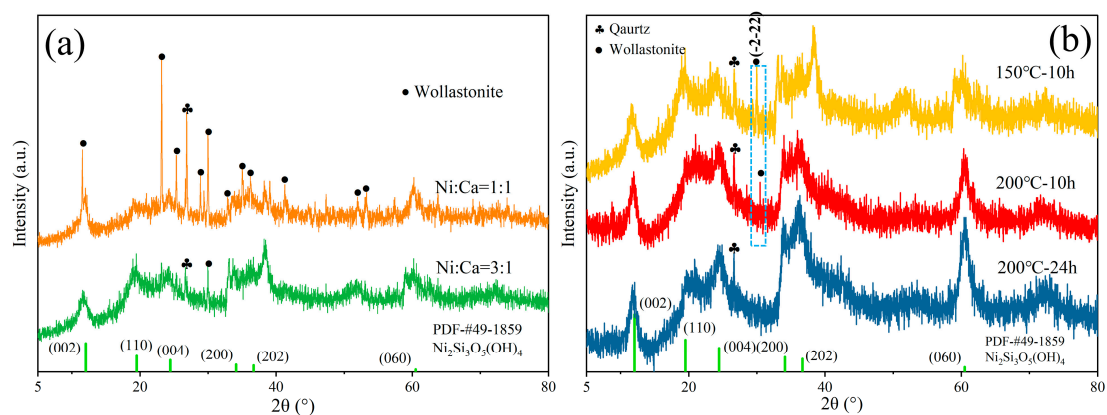


Figure S1. The XRD patterns of $\text{Ni}_3\text{Si}_2\text{O}_5(\text{OH})_4$ prepared under different conditions: (a) different mole ratios of Ni and Ca in wollastonite and (b) different reaction temperatures and times.

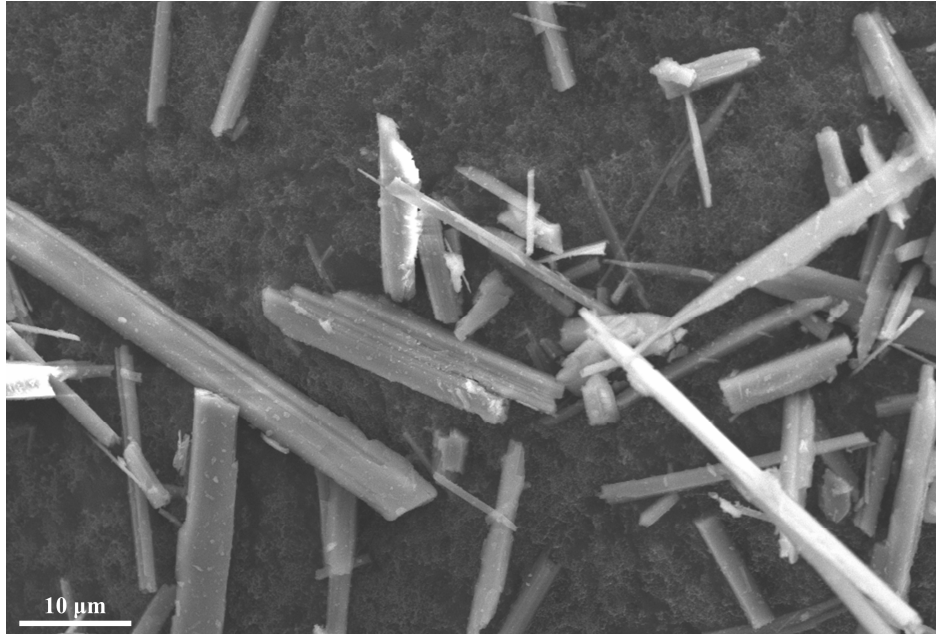


Figure S2. The SEM of wollastonite before the reaction.

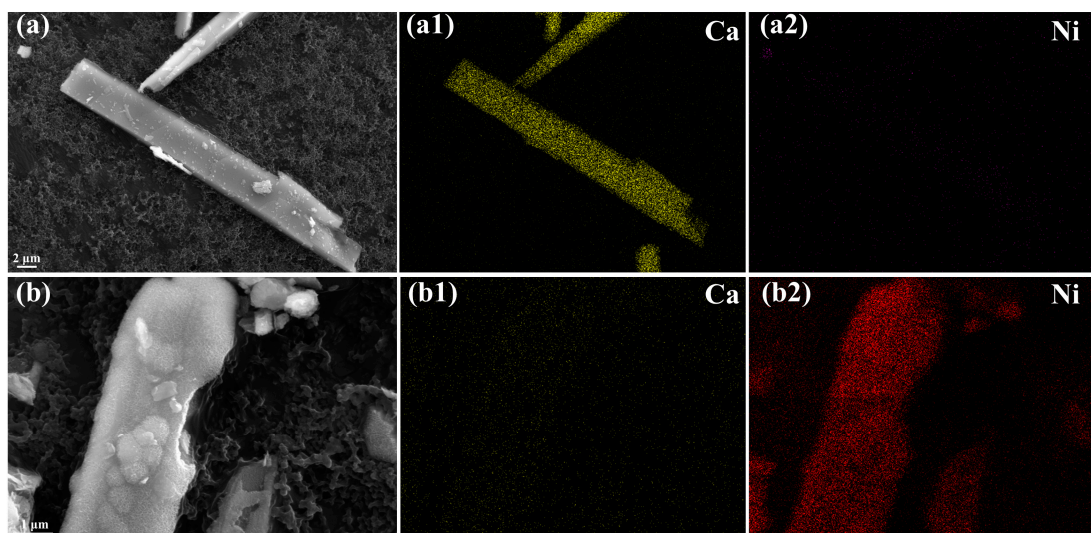


Figure S3. The SEM of wollastonite (a): Ca (a1) and Ni (a2) element distribution of wollastonite (a); the SEM of 3-NS-200-24 (b): Ca (b1) and Ni (b2) element distribution of 3-NS-200-24 (b).

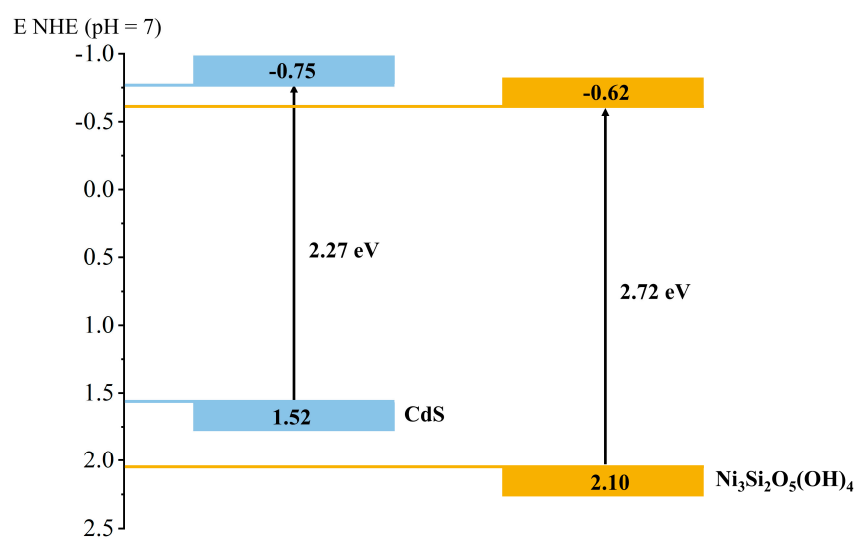


Figure S4. The band structures of CdS and Ni₃Si₂O₅(OH)₄.

Table S1. Specific surface area and pore volume of wollastonite, $\text{Ni}_3\text{Si}_2\text{O}_5(\text{OH})_4$, and CdS/NS.

Samples	S_{BET} (m^2/g)	Pore Volume (cc/g)
Wollastonite	2.25	0.008
$\text{Ni}_3\text{Si}_2\text{O}_5(\text{OH})_4$	178.4	0.276
CdS/NS	137.128	0.385